

Automated comparison of firearm bullets

Fernando Puente León*

Technische Universität München, Lehrstuhl für Messsystem- und Sensortechnik, D-80290 Munich, Germany

Received 11 November 2004; received in revised form 6 December 2004; accepted 29 December 2004
Available online 5 February 2005

Abstract

Fired bullets bear striation marks that can be thought of as a “fingerprint” left by the firearm. This new comparison approach is based on an automated extraction of a “signature” encompassing the relevant marks from an image. To this end, multiple pictures of the bullet are recorded first by using different illumination patterns, and a high quality image is generated by means of fusion techniques. After a preprocessing, the image intensities are filtered along the striations direction, yielding a compact representation of the marks. A non-linear filter selects the striae of interest. The actual comparison takes place by cross-correlating the signatures obtained this way. Finally, an assessment strategy is proposed to objectively evaluate the performance of the system. As demonstrated with an image database of real bullets, the proposed approach outperforms a state-of-the-art commercial system.

© 2005 Elsevier Ireland Ltd. All rights reserved.

Keywords: Firearms identification; Bullet matching; Automated visual inspection; Image comparison; Image fusion; Forensic science

1. Introduction

When a cartridge is fired from a firearm, characteristic marks are left on the surface of the cylindrical section of the bullet. These marks consist of coarse periodic structures that comprise the so-called class marks, related to the class characteristics, as well as fine grooves that form the individual marks. The class marks are characterized by parameters such as the number, width and angle of depressions or “land engravings”, and are representative of the firearm type; see Fig. 1 (left). On the other hand, the individual marks characterize a specific firearm; see Fig. 1 (right). They represent a kind of “fingerprint” of the barrel of the respective gun, and therefore constitute the most relevant evidence in the context of forensic examination. The individual marks are the essential clues to discover and to prove a connection between a bullet and a gun. The ultimate goals of the comparison of bullets are the following:

- The discovery of connections between crimes. This is done by comparing the munitions found at crime scene with the police’s munitions archive.
- The identification of firearms used in crimes. This is accomplished by comparing the munitions of confiscated weapons with the munitions archive.

Considering the amount of orders that are placed for such comparisons, and the size of the police’s munitions archive, in many countries several thousand individual comparisons would be necessary each month. In addition, if more than one munitions archive exists, the need of automation and the advantages of sharing a computerized database of bullets become even more evident.

Currently, the comparison of bullet striae is still often accomplished through visual inspections. Needless to say, this approach is very error-prone and extremely time consuming. Consequently, long queues of requests develop, and the forensic processing of a case may take several months. Moreover, the estimated success rate of identifying firearms is very low in practice. Obviously, the assistance of a computer-based comparison system would be very helpful

* Tel.: +49 89 289 23350; fax: +49 89 289 23348.
E-mail address: f.puente@tum.de.

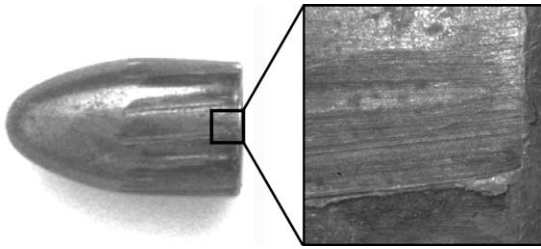


Fig. 1. Firing marks on a bullet.

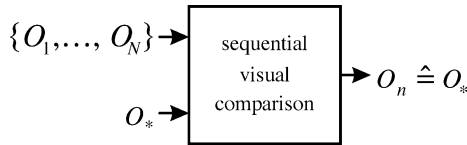


Fig. 2. Visual comparison of the test object O_* with the archive $\{O_1, \dots, O_N\}$. $O_n \hat{=} O_*$ means that O_n shall be deemed to have been fired from the very same firearm as the bullet O_* .

to speed up and ease the work of firearm examiners. The requirements for a useful technical solution to this task comprise

- an automated imaging system that provides high quality images and thorough data acquisition, and which can be performed under easily reproducible conditions,
- the extraction of certain features necessary for a database search,
- the generation of a hit list of possible striae correspondences,
- and finally, a visual comparison of the most likely entries of the hit list, performed by a firearm examiner.

In a formal notation, the firearm examiner gets an exhibit O_* for which he tries to find a counterpart within a munitions archive $\mathcal{M} = \{O_1, \dots, O_N\}$ consisting of N objects O_i featuring the same class characteristics. Without further information, the order of search is arbitrary; see Fig. 2. The desired automation aims to reduce the number n of objects O_i , which must be compared visually with the exhibit O_* until a correspondence is found, assuming that a pendant of O_* is actually present within the archive $\{O_1, \dots, O_N\}$. The final decision is to be reserved to the firearm examiner. He judges whether a match is conclusive or not. Of course, it is

not intended that the examiner be replaced by a computer program but rather to facilitate his work. This is accomplished by sorting the objects O_i of the archive $\{O_1, \dots, O_N\}$ according to their resemblance to the exhibit O_* . The sorted archive $\{O_{(1)}, \dots, O_{(N)}\}$, i.e. the hit list, informs the examiner about the most promising order of potential matches for his visual comparison; see Fig. 3.

The first approaches to automate firearm comparisons by means of image processing were already undertaken in the seventies [1,2]. However, no commercial solutions were available until the early nineties [3]. The signal processing of these approaches is usually based on averaging image intensities along the striations direction to compute a “signature”, which is used for the subsequent database comparison. An important drawback of most systems is that the quality of the raw image data is insufficient. Thus, the overall performance is not always satisfactory [4], despite the continual development of their partly secret algorithms [5]. More recently, further interesting approaches to semi-automated feature extraction from bullet images have been published [6]. However, the performance of such methods significantly depends on the quality of the user input, so that only fully automated solutions shall be considered here. As will be demonstrated in the following, thanks to a high-performance imaging strategy and the reliable extraction of suitable features from the image data, the methods proposed in this paper clearly outperform a well-known state-of-the-art commercial system [3].

It should be mentioned that bullet comparisons could also be accomplished based on 3-D data [4,6,7]. However, suitable profilometers are not only still expensive, but they also lack the desirable degree of maturity to reliably record highly reflecting surfaces showing high slopes. On the other hand, in the case of conventional intensity images, a proper lighting enables a selective, high contrast imaging of the marks of interest. Such images feature the crucial advantage of an easier visual interpretability, which also leads to a higher court acceptance. For all of these reasons, intensity images remain indispensable, whereas 3-D data represent a valuable complement to be exploited.

2. Imaging and fusion

In forensic science, a reliable and reproducible imaging of the finest marks is necessary. Therefore, great strides must

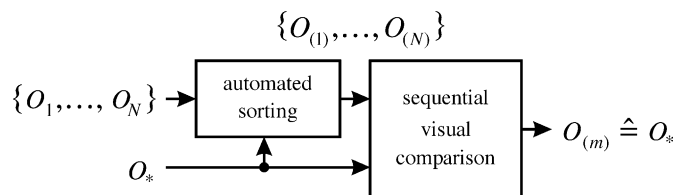


Fig. 3. Searching along the sequence suggested by the computer. On the average, the number m of visual comparisons until the hit ($O_{(m)} \hat{=} O_*$) is found should be distinctly smaller than n .

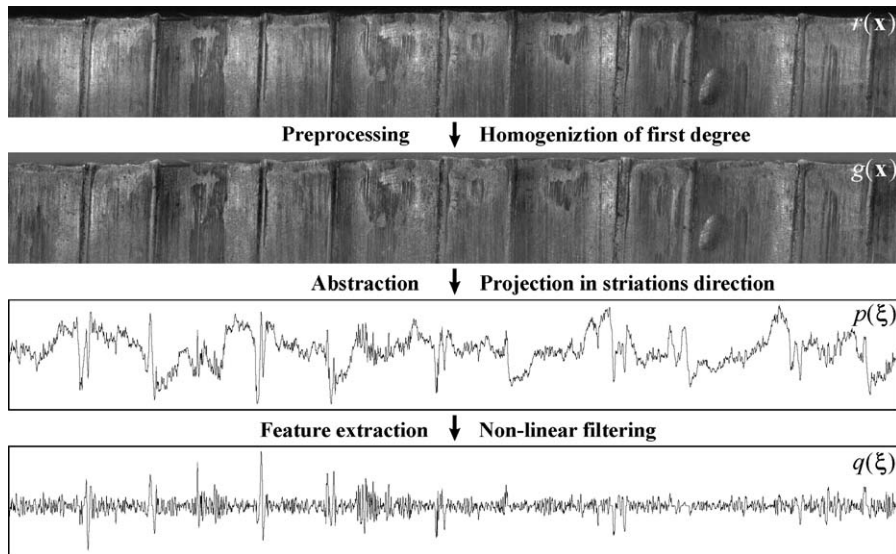


Fig. 4. Processing strategy to generate a signature.

be made in the area of image capture. Particularly, high image sharpness, high contrast, and a thorough coverage of the cylindrical surface of the bullet are needed. These requirements can be fulfilled by acquiring a series of images $\mathcal{D} = \{d(\mathbf{x}, \omega_i), i = 0, \dots, B - 1\}$ (1)

in which the object distance, the illumination direction, and the rotational position of the bullet are all varied, and a subsequent multidimensional image fusion is performed [8]. The image series \mathcal{D} is characterized by a parameter vector $\omega = (\phi, \theta, \zeta, \alpha^T)$ describing the recording situation, where ϕ and θ represent the azimuth and the elevation angle of the illumination direction, respectively, ζ denotes the object distance, and α^T the object pose with respect to the imaging system. The result of the fusion is an image $r(\mathbf{x})$ that exhibits high sharpness and contrast, where $\mathbf{x} = (x, y)^T \in \mathbb{R}^2$ denotes the location vector. An example is shown at the top of Fig. 4. In this case, the data acquisition was fully automated, and it provides an image size of 8192×512 pixels.¹ The remaining processing strategy presented in this figure is addressed in Section 3.

2.1. Image capture

An important question when recording an image series deals with the strategy to sample the parameter space ω with as few images as possible, such that (1) every surface location \mathbf{x} is imaged with high quality at least once in the series, and (2) fusion to an improved result $r(\mathbf{x})$ is possible. This problem highly depends on the object geometry as well as on the surface texture and cannot be dealt with in detail

¹ The time needed to acquire such an image of a single undamaged bullet, and to process the data according to Sections 3 and 4 is less than 1 min.

here. However, the following cases relevant to imaging of bullets will be treated in more detail:

- Cylindrical surfaces showing a single band of straight, parallel grooves, such as pristine bullets, only show a high contrast, if illumination is perpendicular to the grooves [9]. Thus, only the elevation angle θ of the illumination direction has to be varied. If the interesting surface areas are not all in-focus simultaneously, the object distance ζ should be varied, too.
- When dealing with non-planar surfaces containing curved grooves, such as deformed bullets, the elevation angle θ as well as the azimuth ϕ of the light source have all to be varied to assure locally a high quality in at least one image of the series. Additionally, the object distance ζ and the object pose α^T may have to be varied as well to achieve a proper focusing and low distortions.
- To provide for a thorough coverage of the cylindrical surface of a bullet, a series of images is obtained by rotating the bullet by a certain angular increment. If the images obtained partly overlap, they can precisely be concatenated by means of correlation methods [10].

2.2. Fusion strategy

After an image series \mathcal{D} has been acquired, the information of interest distributed over the series is combined to an enhanced result $r(\mathbf{x})$ showing overall a high quality. Such a result is not only advantageous to perform a computerized comparison, but it can also be used to support firearm examiners in matching of striae, because a larger area of the bullet surface can be visualized simultaneously with high contrast as compared with conventional comparison microscopes. Fig. 5 shows the fusion algorithm for the case of a

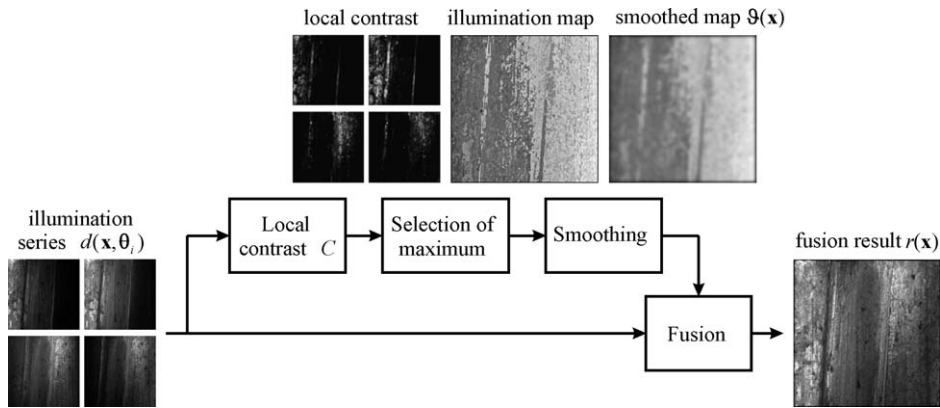


Fig. 5. Structure of the algorithm for fusing illumination series.

varying elevation angle θ . By applying the same method in several stages, multidimensional series of images can also be fused [9].

The principle of the algorithm consists in selecting the best-illuminated image segments of the series for each location \mathbf{x} based on the maximization of a local criterion C . Since in our case a high contrast is desired, the local gray level variance and the local entropy are suitable criteria C . The selected illumination direction maximizing the contrast, which is stored for each location \mathbf{x} in the so-called illumination map

$$\hat{\vartheta}(\mathbf{x}) = \arg \max_{\theta_i} C\{d(\mathbf{x}, \theta_i)\}, \quad (2)$$

has to be a spatial function varying slowly compared with the signal of interest, i.e. the width of the marks. This is necessary to avoid artifacts in the fusion result. To assure that this condition is satisfied, a smoothing of $\hat{\vartheta}(\mathbf{x})$ is performed with a low-pass filter: $\vartheta(\mathbf{x}) = LP\{\hat{\vartheta}(\mathbf{x})\}$.

The actual fusion is performed by a weighted superposition of two adjacent images $d(\mathbf{x}, \theta_i)$ by means of a linear interpolator γ taking the “best” local illumination direction $\vartheta(\mathbf{x})$ into account:

$$\begin{aligned} r(\mathbf{x}) &= \sum_i d(\mathbf{x}, \theta_i) \gamma(\vartheta(\mathbf{x}) - \theta_i) \\ &= \frac{\vartheta(\mathbf{x}) - \theta_l}{\theta_{l+1} - \theta_l} d(\mathbf{x}, \theta_l) + \frac{\theta_{l+1} - \vartheta(\mathbf{x})}{\theta_{l+1} - \theta_l} d(\mathbf{x}, \theta_{l+1}). \end{aligned} \quad (3)$$

The interpolation takes care of a smooth transition between θ -neighboring images. The narrow extent of γ provides for an averaging of only similarly illuminated images. Thus, an undesirable contrast loss due to destructive interferences of light and shadow is avoided.

Three properties of the proposed fusion method are responsible of its good performance: (1) the fusion result $r(\mathbf{x})$ resembles locally the best illuminated image $d(\mathbf{x}, \theta_i)$ of the series; (2) the smoothness of the selected illumination direction $\vartheta(\mathbf{x})$ guarantees that no artifacts are contained in the resulting image $r(\mathbf{x})$; (3) the result achieves globally good results in the sense of maximizing the local contrast C .

3. Processing strategy

Once suitable images $r(\mathbf{x})$ have been generated, the signal processing scheme according to Fig. 4 is employed to generate a signature.

The preprocessing suppresses texture inhomogeneities that arise from the illumination and from the object shape while simplifying the further signal processing. For this purpose, a directional Gaussian high-pass filter that provides for a homogenization of first degree—i.e. of the local average gray level—is used to eliminate low-frequency signal fluctuations perpendicular to the grooves without generating undesirable artifacts [11,12]. Fig. 4 presents an example of the preprocessing: at the top, the fusion result $r(\mathbf{x})$ is shown; directly below the result $g(\mathbf{x})$ of the homogenization is depicted.

The abstraction aims to reduce the data by incorporating a priori knowledge on the signal formation. Due to the kinematics of the firing process, all individual peculiarities in the barrel of a gun are mapped onto grooves. Consequently, all gray level fluctuations along grooves necessarily must be disturbances. By means of averaging, these disturbances can efficiently be suppressed; see Fig. 6. In the case of pristine bullets, straight grooves can be assumed, and their angle ψ is estimated in the Fourier domain [13]. However, if a bullet is deformed, the grooves are usually curved. In this case, for each location \mathbf{x} the local orientation $\psi(\mathbf{x})$ is estimated first, and then a non-linear coordinate transform is performed to straighten the grooves [13]. In either case, the final step is to carry out a projection along the striations direction. Since the result of the preprocessing was a zero-mean signal, it is not necessary to exclude blank areas without striae to avoid an undesirable averaging of individual characteristics. The resulting projection signal $p(\xi)$ describes the intensity profile of the grooves. An important advantage of this abstraction approach is the considerable reduction of the amount of data needed to describe the relevant marks, which contributes to the efficiency of the ulterior comparison.

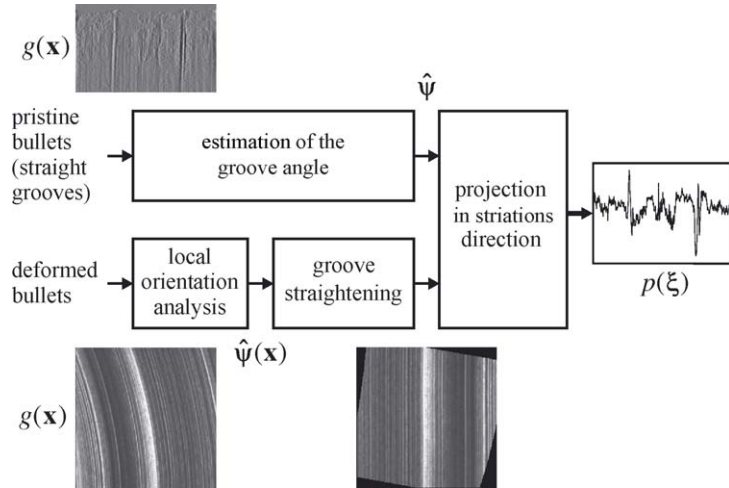


Fig. 6. Processing scheme for the abstraction.

Following, features describing the relevant marks are extracted from the abstraction result $p(\xi)$. A compact representation of the signal of interest is obtained which contains all individual information needed to perform a reliable comparison, as described in Section 4.

Finally, the feature set obtained this way is compared with all eligible data sets stored in the munitions database using proper feature metrics; see Section 5. This results in a distance measure directly suited for an automated sorting of the munitions archive. Section 6 introduces a concentration measure that enables a quantitative assessment of the proposed methodology. To conclude the paper, experimental results obtained with the presented approach are discussed in Section 7.

4. Feature extraction

In the preceding section, an abstraction strategy to obtain a compact description of the essential signal components of bullet images has been presented. In the resulting signal $p(\xi)$, information concerning class features as well as individual features are overlaid:

- Class features related to the caliber, the angle of twist, and the shape of the land engravings, which are generated by the rifling of the barrel, all constitute signal disturbances or noise that we wish to ignore.
- Individual features are essentially the location and distinctness of fine structures, and they represent the information of interest.

Thus, the projection $p(\xi)$ is not suited for an immediate comparison. Instead, a selective extraction of the individual features has to be performed. For this purpose, morphological methods are especially suited [14].

Morphological methods originate from the application of set theory operations to image analysis [15]. They are based on non-linear transforms, within which signals are represented as sets.² By properly choosing a structuring element $s(\xi)$, knowledge concerning the shape of the signals of interest can selectively be incorporated into morphological filters, thus enabling a selective separation of different signal components.

The top-hat transform is a well-known morphological operator to detect subtle structures [14]. Depending on whether bright or dark structures are to be detected, two different variants exist:

$$q_b(\xi) := p(\xi) - p(\xi) \circ s(\xi), \quad (4)$$

$$q_d := p(\xi) \bullet s(\xi) - p(\xi), \quad (5)$$

where $s(\xi)$ represents a planar structuring element of width $|\Omega_s|$, and $\Omega_s := \text{supp}\{s(\xi)\}$ specifies its support set. The operators \circ and \bullet denote a morphological opening and a closing, respectively [14]. The results of these transforms are signals $q_b(\xi)$ and $q_d(\xi)$ indicating the location and distinctness of fine bright or dark peaks, which in the projection $p(\xi)$ stand for the grooves, as shown in the examples of Fig. 7(a and b). The dotted lines represent the opening and the closing of $p(\xi)$, respectively. At the bottom, the results of both variants of the top-hat transform are depicted.

If now the difference between $q_b(\xi)$ and $q_d(\xi)$ is calculated, one obtains a signal containing only fine peaks, while the coarser structures—which mainly describe class features—are suppressed:

$$q(\xi) := q_b(\xi) - q_d(\xi). \quad (6)$$

Just like a linear high-pass filter eliminates low frequencies corresponding to wider structures, Eq. (6) lets pass only

² For the sake of consistency, all signals throughout this paper are represented by means of lower-case letters instead of using capital letters as in set theory.

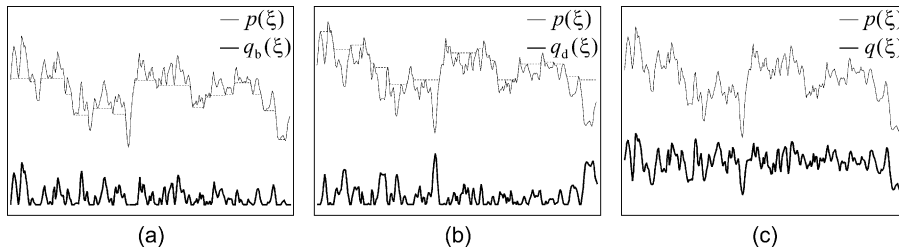


Fig. 7. Morphological top-hat transform of a segment of a bullet projection $p(\xi)$: (a) bright structures $q_b(\xi)$; (b) dark structures $q_d(\xi)$; (c) result $q(\xi)$ of the morphological filtering (signature).

signal components that are narrow enough in space domain. For this reason, Eq. (6) can be thought of as a kind of “non-linear high-pass filter”, where by choosing the width $|\Omega_s|$ of the structuring element $s(\xi)$ the limit between the structures to be preserved and those to be suppressed can be selected. Because this procedure leads to an efficient elimination of class features, the resulting signal $q(\xi)$ is well suited for a comparison of individual marks.

In the example shown in Fig. 7(c), the result $q(\xi)$ only consists of fine peaks and, thus, it represents the information relevant to the comparison. In a further example depicted in Fig. 4, the performance of this filter can clearly be recognized. Whereas the periodic signal components describing the class characteristics are still visible in the projection $p(\xi)$, they cannot be recognized anymore after the feature extraction. Since the filtered signal $q(\xi)$ describes the signal of interest efficiently, and it is relatively simple to extract, it constitutes a suitable “signature” for the comparison of individual marks and will be used as the basis of the following comparison.

5. Comparison

In the actual comparison stage, the similarity of two signatures $q_1(\xi)$ and $q_2(\xi)$ describing different bullets O_1 and O_2 has to be examined quantitatively by means of a suitable distance measure $d(q_1(\xi), q_2(\xi))$. In such cases, methods based on the empirical cross-correlation function (CCF)

$$k_{12}(\tau) := \bar{q}_1(\xi) \times \bar{q}_2(\xi) = \int_{-\infty}^{\infty} \bar{q}_1(\xi) \bar{q}_2(\xi - \tau) d\xi \quad (7)$$

of the signals $\bar{q}_1(\xi)$ and $\bar{q}_2(\xi)$ are especially advisable, where $\bar{q}_1(\xi) := (q_1(\xi) - m_{q_1})s_{q_1}^{-1}$ and $\bar{q}_2(\xi) := (q_2(\xi) - m_{q_2})s_{q_2}^{-1}$ denote the signals centered around their mean values m_{q_i} and normalized with $s_{q_i} := \sqrt{\text{var}\{q_i(\xi)\}}$ to have a standard deviation of one. The location of the maximum of the CCF $k_{12}(\tau)$ indicates the shift τ_0 leading to the best match between the images of the two bullets:

$$\tau_0 := \arg \max_{\tau} \{k_{12}(\tau)\}. \quad (8)$$

The knowledge of this shift can contribute to a reduction of the time needed by a firearm examiner to accomplish a visual

evaluation of possible connections between two different striation patterns.

To sort the munitions archive, a comparison of the exhibit O_* with each bullet stored in the corresponding database is performed. The result of the database search is visualized in form of a hit list indicating potential striation correspondences at the top of it. To determine the order of the list, a feature ρ_{12} is needed specifying the similarity between two bullets quantitatively. It is straightforward to use the maximum of the CCF:

$$\rho_{12} := \max \{k_{12}(\tau)\}. \quad (9)$$

Though the cross-correlation coefficient ρ_{12} does not represent a metric for the existing diversity between the signals $\bar{q}_1(\xi)$ and $\bar{q}_2(\xi)$, it should be emphasized that the sorting of a munitions archive based on ρ_{12} leads to the same results as if an actual metric had been used [13].

Fig. 8 illustrates the proposed strategy with an example. In the upper area, the signals $q_1(\xi)$ and $q_2(\xi)$ resulting from the feature extraction of the images of two different bullets are shown. In the center, the CCF $k_{12}(\tau)$ is depicted, the maximum of which reveals the displacement τ_0 of both signals. At the bottom, the corresponding images $r_1(\mathbf{x})$ and $r_2(\mathbf{x})$ are represented, shifted by the distance τ_0 . Even a layman can recognize at once the great similarity of both bullets, which indeed were fired from the same gun.

Fig. 9 presents further examples of typical CCFs. The three signals on the left side originate from projectiles, which were fired from the same gun—all of them show pronounced maxima. In the other plots, which describe bullets from different guns, no distinct peaks can be recognized. In the context of investigations of bullets showing well-pronounced marks, the determination of whether two bullets were fired from the same gun, when based on the cross-correlation coefficient ρ_{12} , was always successful. In this manner, the aptitude of this feature to determine the similarity of two bullets quantitatively was experimentally verified.

One may object that values of the coefficient ρ_{12} lower than 0.5, such as those obtained in the present cases, are too low to permit a reliable identification. However, given the actual variations of the diameters, material and amount of gunpowder of different munitions, it should not surprise anyone that the similarities between bullets fired from the

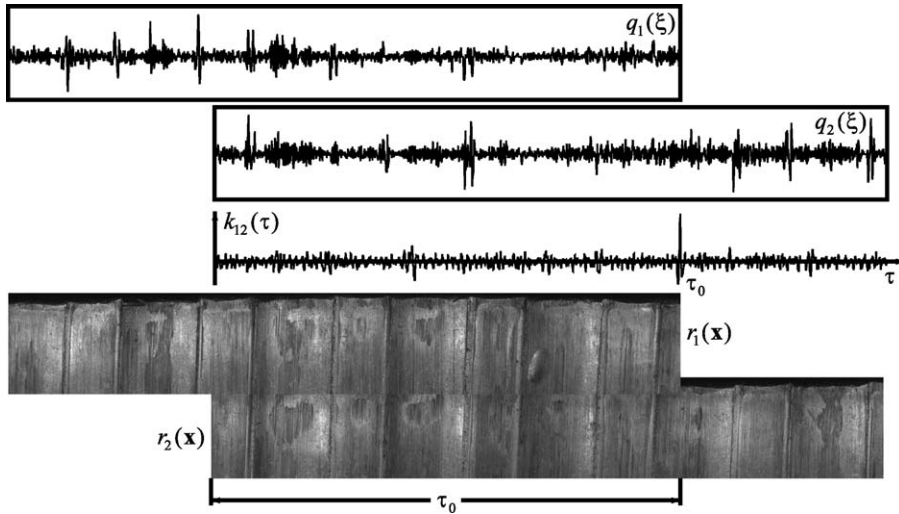


Fig. 8. Example of a bullet-to-bullet comparison.

same weapon can often just barely be recognized by forensic experts. Consequently, the low degrees of likeness achievable reflect the intrinsic difficulty of firearms identification.

Eq. (7) can be implemented very efficiently in the frequency domain by means of the FFT algorithm. The periodic continuation of the signals inherent to the discrete Fourier transform does not impair the result of the computation, because in this case the signals $\tilde{q}_i(\xi)$ are actually cyclic. An important advantage of the proposed methodology is its low computational expense: the computing time required for the correlation of two signatures is in the order of 1 ms. An additional advantage of this approach is that, as a matter of principle, it also enables a comparison of signatures extracted with alternative methods—provided that these are conveniently represented as signals $q_i(\xi)$; see [2,1]—although in this case, due to the differences in the processing of the data, optimal results should not be expected.

Finally, it should be emphasized that the CCF only registers linear similarities between signals or processes. A substantially more general approach, which stems from

information theory and allows the investigation of arbitrary types of statistical dependence, is based on the computation of the cross-entropy function (CEF). Unfortunately, the price of the generality of this alternative approach is that the CEF yields a lower information gain than the CCF, if the statistical dependence is essentially linear [10].

6. Assessment

By means of the strategy introduced, a hit list providing a suitable order $\{O_{(1)}, \dots, O_{(N)}\}$ of the munitions archive can be created for an exhibit O_* . This section presents a method to assess the overall performance of the system. Since on the average, a high concentration of bullets fired from the same gun as the exhibit O_* on the first positions of the hit list is desired, the assessment is based on a measure of concentration [16].

A particularly clear possibility of representing concentration is graphically in the form of a so-called concentra-

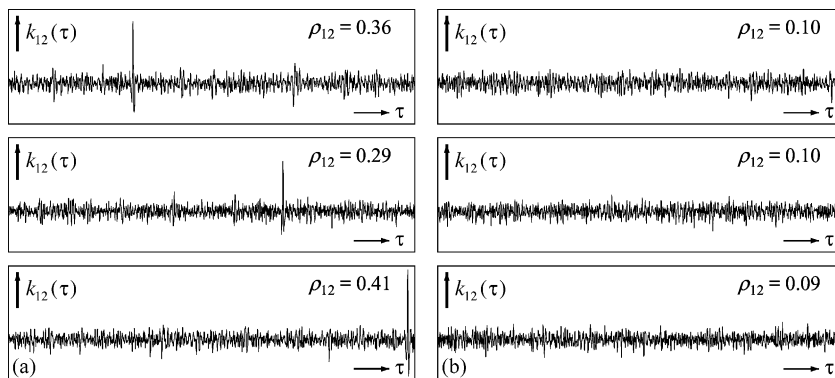


Fig. 9. Cross-correlation functions $k_{12}(\tau)$ and corresponding coefficients ρ_{12} : (a) bullets from the same gun; (b) bullets from different guns.

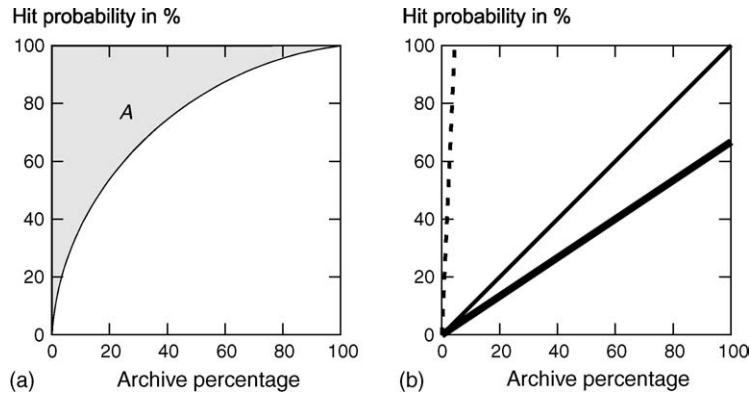


Fig. 10. Concentration curves: (a) illustration of the principle; (b) probability of finding an actual correspondence for an ideal (thin line) and real (bold line) firearm examiner, as well as for an ideal automated system (dotted line).

tion curve; see Fig. 10(a). For each relative position of the hit list, this curve indicates the probability of finding an actually existing hit, if the hit list is examined just up to this position. It represents a relative cumulative frequency distribution—i.e. an empirical distribution function—for the finding of an existing hit in an archive. The concentration curve is obtained by plotting the cumulative hit rate over the percentage of the archive searched. It represents a monotonic growing function, which in case of a missing concentration of hits in the hit lists generated by a system, coincides with the bisector. The more the shape of the concentration curve differs from the bisector up to the left upper side, the bigger is the concentration of hits within the first positions of a typical hit list and the better the performance of the system.

A concentration measure commonly used in statistics is the Rosenbluth index [16]: $K_R = 1/(2A)$, where A denotes the grayed area above the curve in Fig. 10(a). It constitutes a measure for the bulge of the concentration curve. To achieve a high concentration of hits on the first positions of the hit lists, the area A has to be minimized. Since A describes the portion of the archive to be examined on the average until an actually existing match is found, an immediately clear interpretation of the concentration curve is obtained.

To illustrate the meaning of the concentration curve, Fig. 10(b) shows three examples, each one describing the probability of finding an actual striae correspondence in an archive based on different assumptions. The thin line represents the ideal firearm examiner, who is able to compare marks without errors and does not overlook any correspondence. Consequently, the probability of finding the existing match grows linearly, and reaches the value 100% as soon as the whole archive has been scrutinized. The real firearm examiner, however, overlooks mark correspondences. Accordingly, the corresponding concentration curve (bold line) does not reach the value 100% even after having processed the whole archive. The dotted line describes the ideal automated comparison system, which distinguishes itself by always placing the matching bullet at the first

position of the hit list. In this case, a firearm examiner would just have to check one munitions piece, which would lead to the highest possible reduction of the comparison effort.

It should be pointed out that the firearm examiner—even when being supported by an automated system—will continue to play an essential role within the comparison process. Therefore, in practice the characteristics of their respective concentration curves should be taken into account simultaneously. Moreover, one cannot necessarily expect from an automated system to increase the success rate of finding actual striae matches. The purpose of such a system is rather to reduce the time needed for manual comparison without affecting the quality of the search substantially.

To assess the presented algorithms quantitatively, a specific munitions archive \mathcal{M} has been generated for which the actual correspondences between the bullets and the firearms used to fire them were known beforehand. Following, series of images of all the bullets $O_i \in \mathcal{M}$ have been acquired and fused to high quality images with the methods described in Section 2, where $\mathcal{M} = \cup_f \mathcal{W}_f$ denotes the set of all bullets in the archive, and \mathcal{W}_f describes the bullets fired from a specific firearm f . By processing of the images according to Sections 3 and 4, signatures have been extracted and stored in a database.

To calculate the concentration curve and to compute the quality measure A , each bullet $O_i \in \mathcal{W}_f \subset \mathcal{M}$ is regarded as an exhibit and is compared with every remaining projectile $O_j \in \mathcal{M}$, $j \neq i$, of the database. This way, for each test bullet O_i a hit list is created. In a formal way, the hit list for the test projectile O_i is described by means of the mapping $k = L_i(r)$, which associates each rank $r \in \{1, \dots, N\}$ of the hit list—i.e. each object $O_{(r)}$ of the sorted archive according to Fig. 3—with the index k of the corresponding munitions piece O_k . Following, the relative rank

$$r_i(k) := \frac{\tilde{L}_i^{-1}(k)}{|\mathcal{M}| - |\mathcal{W}_f| + 1} \quad (10)$$

of each bullet $O_k \in \mathcal{W}_f$ of $\tilde{L}_i(r)$ matching the exhibit O_i is determined, where $\tilde{L}_i(r)$ denotes a modified hit list generated from $L_i(r)$ by deleting all items l ($l \neq k$) describing bullets $O_l \in \mathcal{W}_f$ originating from the same firearm f as the bullet O_i . By analyzing all combinations of bullets from the same guns in the database, the empirical distribution density $p_r(r)$ of the relative ranks $r_i(k)$ is obtained as follows:

$$p_r(r) := \frac{\tilde{p}_r(r)}{\int_0^1 \tilde{p}_r(\beta) d\beta} = \frac{\tilde{p}_r(r)}{Z} \quad (11)$$

with

$$\tilde{p}_r(r) := \sum_{\mathcal{W}_f \subset \mathcal{M}} \sum_{O_i, O_k \in \mathcal{W}_f, i \neq k} \delta_r^{r_i(k)} \delta(r - r_i(k)), \quad (12)$$

where

$$Z := \sum_{\mathcal{W}_f \subset \mathcal{M}} 2 \binom{|\mathcal{W}_f|}{2} = \sum_{\mathcal{W}_f \subset \mathcal{M}} |\mathcal{W}_f| (|\mathcal{W}_f| - 1) \quad (13)$$

indicates the total number of bullet combinations from the same guns, and

$$\delta_a^b := \begin{cases} 1 & \text{for } a = b \\ 0 & \text{for } a \neq b \end{cases} \quad (14)$$

denotes the Kronecker symbol. Eq. (11) solely takes care of normalizing the density $\tilde{p}_r(r)$ to the value of one. The multiplication with the $\delta(\cdot)$ function in Eq. (12) provides for a value greater than zero after integrating the density $\tilde{p}_r(r)$, thus avoiding a division by zero in Eq. (11). Integration of Eq. (11) yields immediately the concentration curve as the cumulative distribution

$$P_r(\chi) := \int_0^\chi p_r(r) dr. \quad (15)$$

Finally, the area A can be computed as the percentage of the archive to be examined on the average until the actual match is found:

$$A := \frac{1}{Z} \sum_{\mathcal{W}_f \subset \mathcal{M}} \sum_{O_i, O_k \in \mathcal{W}_f, i \neq k} r_i(k). \quad (16)$$

The area A represents a global measure to describe concentration. Thus, it is straightforward not only to utilize the Rosenbluth index K_R —which is proportional to the reciprocal value of A —as a quality measure, but also to maximize it with respect to the different algorithmic alternatives available and to their respective tuning parameters. This way, the need of performing a homogenization to preprocess the data could be verified experimentally, and the optimal dimensioning of the corresponding one-dimensional Gaussian resulted in a standard deviation of $\sigma = 4$. Similarly, the aptitude of the morphological top-hat transform to extract individual features was also confirmed. Here, the choice of a planar structuring element of width $|\Omega_s| = 23$ ($\cong 80 \mu\text{m}$) appeared as especially favorable, although the method showed a fairly robust behavior with respect to small variations of this parameter. These settings were used in the experiments described in the following.

7. Experimental results

This section presents results achieved by the proposed system as well as those attained by the state-of-the-art commercial system IBIS [3]. The open case file used was generated by firing several 9 mm luger caliber pistols with ammunition from different manufacturers; see Table 1. For all subsequent comparisons, the same database consisting of 27 bullets from 12 different guns was used. Fig. 11 shows the resulting concentration curves for both systems. As can be seen, the strategy described in this paper performs the best, although the commercial system also leads to a relatively small area above the curve. The value of the concentration measure A is 14.7% for our system, and 27.2 for the commercial system.

Table 1
Ammunition and guns of the open case file

No.	Manufacturer	Quality of marks	Gun
1	Geco	Fair	
2	Lapua	Fair	FN Mod. 35
3	R-P	Good	
4	DAG	Good	
5	DAG-SX	Good	DWM Mod. 08
6	SBP	Good	
7	Geco	Good	
8	MEN	Fair	Walther Mod. P38
9	MEN	Good	
10	Sintox	Fair	Ceska Mod. 75
11	Sintox	Good	
12	DAG-SX	Good	FN Mod. HP
13	Geco	Good	
14	Sintox	Fair	FN Mod. HP
15	Sintox	Fair	
16	Geco	Good	FN Mod. GP
17	Geco	Fair	
18	Geco	Fair	Mauser Mod. 08
19	Geco	Good	
20	Geco	Fair	Mauser Mod. 08
21	Geco	Fair	
22	DAG-SX	Good	MP 40
23	Winchester	Fair	
24	Sintox	Fair	MP 40
25	Sintox	Fair	
26	Sintox	Fair	Pistole 08
27	Sintox	Good	

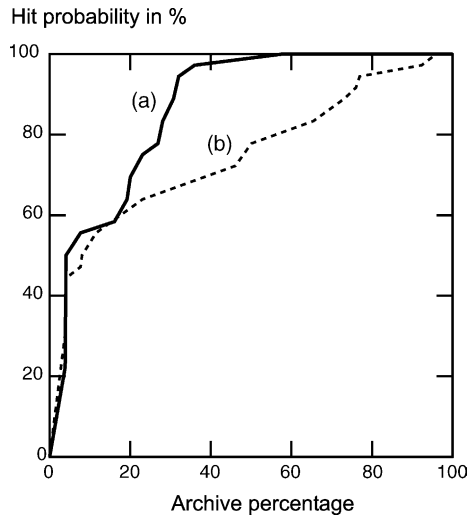


Fig. 11. Results of the bullet comparison with experimental data: (a) proposed strategy; (b) commercial system IBIS.

These results demonstrate that—despite the fact that visual recognition of actual correspondences is frequently difficult—the proposed strategy results in a remarkable concentration of hits on the first positions of the hit lists. Indeed, with the database used it is sufficient to check the first position of the hit list to find an actual match with a probability of 50%. If, on the average, 90% of the correspondences are to be found, it will suffice to examine 32% of the munitions archive, which represents almost only a third of the original, purely manual comparison effort.

8. Conclusion

This paper has presented a method by which the comparison of bullets based on gray level images can be automated, thus facilitating the identification of firearms. Such images contain groove-shaped marks that can be thought of as a kind of “fingerprint” left by the firearm on the cylindrical surface of the bullet. To accomplish the comparison task, mainly the fine grooves on the bullet surface are of interest.

The presented approach is based on an automated extraction of a feature set or “signature” describing the relevant marks. To enable a reliable extraction of features, high quality images of the bullets are generated by means of image fusion techniques. After a preprocessing, in which a spatial homogenization of the local average gray level is performed, a model-based abstraction is accomplished by performing a projection of the image intensities of relevant grooves in striations direction. The resulting one-dimensional signals are not only very compact; they also have proven to provide a faithful representation of the surface information originating from the rifling of the firearm. A powerful morphological filter is then employed to separate

those signal components describing the class characteristics—such as the land engravings—from the individual marks of interest. Finally, a strategy for efficiently comparing the resulting signatures has been described.

The performance of the presented system has been demonstrated and quantitatively assessed using an image database of real bullets. Moreover, using test munitions, we were able to undertake an objective comparison of the system with a popular commercial system. Particularly, significantly better results were obtained with the proposed strategy than those attained by the competing system. It has been shown that with these methods, the efficiency of firearms identification can be dramatically increased. Finally, it is worth to mention that most of the methods developed here can be easily transferred to related areas, such as the analysis of cartridge cases, tool marks [13], and even the identification of persons based on relief’s taken of their fingerprints.

Acknowledgments

The author would like to thank Ruprecht Nennstiel and Jürgen Rahm for helpful discussions on the work presented in this paper. He would also like to thank Joshua Cohen, Michael Heizmann, and Prof. Franz Mesch for valuable comments on a draft version of this paper.

References

- [1] W. Deinet, Studies of models of striated marks generated by random processes, *J. Forensic Sci.* 26 (1) (1981) 35–50.
- [2] G.Y. Gardner, Computer identification of bullets, *IEEE Trans. Syst. Man Cybern.* 8 (1) (1978) 69–76.
- [3] R.E. Tontarski, R.M. Thompson, Automated firearms evidence comparison: a forensic tool for firearms identification—an update, *J. Forensic Sci.* 43 (3) (1998) 641–647.
- [4] B. Bachrach, Development of a 3D-based automated firearms evidence comparison system, *J. Forensic Sci.* 47 (6) (2002).
- [5] R. Baldur, Method and apparatus for obtaining a signature from a fired bullet, US Patent 6,219,437 B1, (2001).
- [6] M. Pirlot, A. Chabottier, E. Celens, J. De Kinder, P. Van Ham, Feature extraction of optical projectiles images, *Sci. Justice* 39 (1) (1999) 53–56.
- [7] A. Banno, T. Masuda, K. Ikeuchi, Three-dimensional visualization and comparison of impressions on fired bullets, *Forensic Sci. Int.* 140 (2004) 233–240.
- [8] M. Heizmann, F. Puente León, Imaging and analysis of forensic striation marks, *Opt. Eng.* 42 (12) (2003) 3423–3432.
- [9] F. Puente León, Enhanced imaging by fusion of illumination series, in: *Sensors, Sensor Systems, and Sensor Data Processing*, Proc. SPIE 3100, 1997 pp. 297–308.
- [10] F. Puente León, M. Heizmann, Strategies to detect non-linear similarities by means of correlation methods, in: *Intelligent Robots and Computer Vision XX: Algorithms, Techniques, and Active Vision*, Proc. SPIE 4572, 2001 513–524.
- [11] T. Lindeberg, *Scale-space Theory in Computer Vision*, Kluwer Academic Publishers, Boston, 1994

- [12] J. Beyerer, F. Puente León, Suppression of inhomogeneities in images of textured surfaces, *Opt. Eng.* 36 (1) (1997) 85–93.
- [13] M. Heizmann, *Auswertung von forensischen Riefenspuren mittels automatischer Sichtprüfung*, Karlsruhe University Press, Karlsruhe, 2004.
- [14] R.M. Haralick, L.G. Shapiro, *Computer and Robot Vision*, Addison-Wesley, Reading, MA, 1992.
- [15] J. Serra, *Image Analysis and Mathematical Morphology*, Academic Press, London, 1982.
- [16] P. von der Lippe, *Deskriptive Statistik*, G. Fischer Verlag, Stuttgart, 1993.